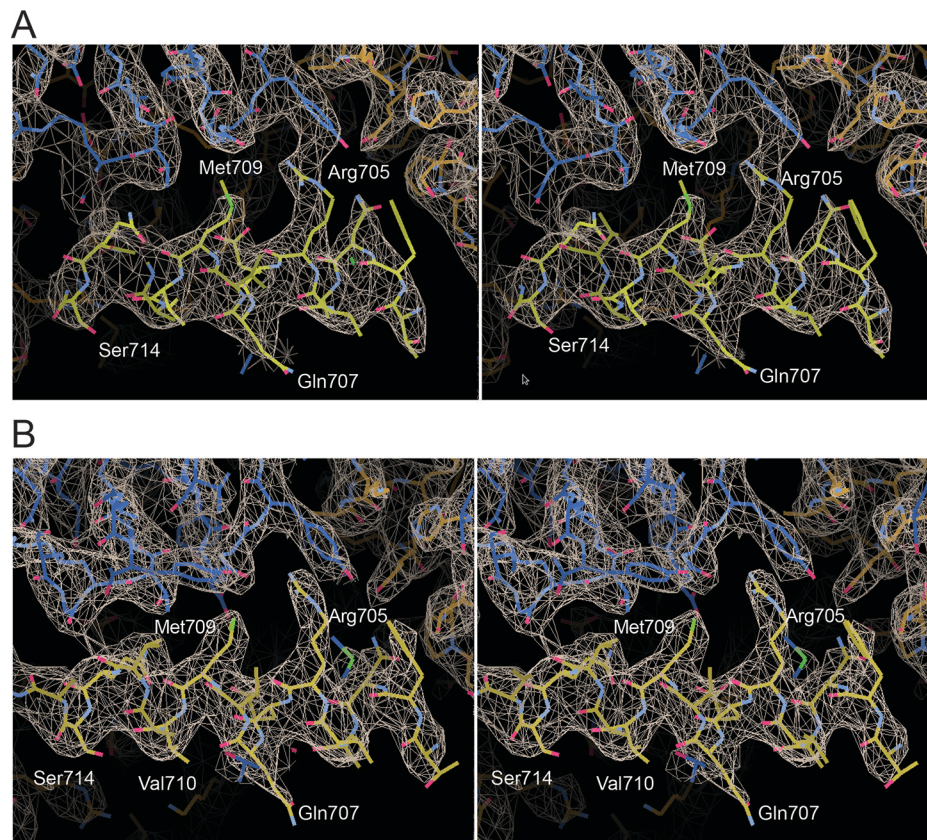
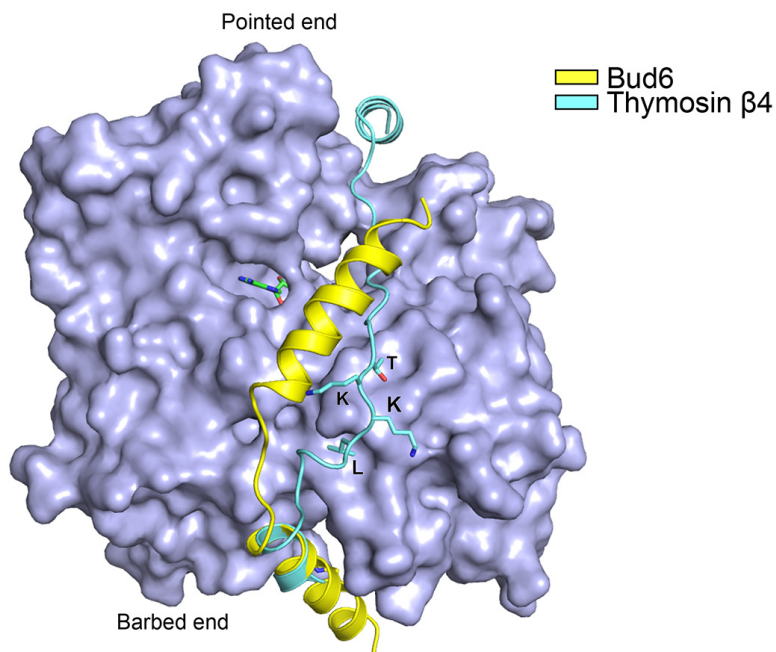


## Supplemental Figures



**Figure S1. Stereo views of electron density maps in the region of Helix  $\alpha$ A of Bud6, related to Figure 1.** A, Experimental electron density map obtained after phase improvement by iterative non-crystallographic symmetry averaging. Starting phases were obtained from the molecular replacement model, which contained only actin. B, 2Fo-Fc electron density map calculated using phases derived from the final model. In both A and B, the final refined model is shown and both maps are contoured at  $1.3 \sigma$ .



**Figure S2. Superposition of Bud6<sup>flank</sup> and the thymosin  $\beta 4$  WH2 domain bound to actin, related to Figure 2.** The “LKKKT” sequence motif found in thymosin  $\beta 4$  and other WH2 domains is shown in a stick representation. The thymosin  $\beta 4$  structure is drawn from PDB ID 4PL7.

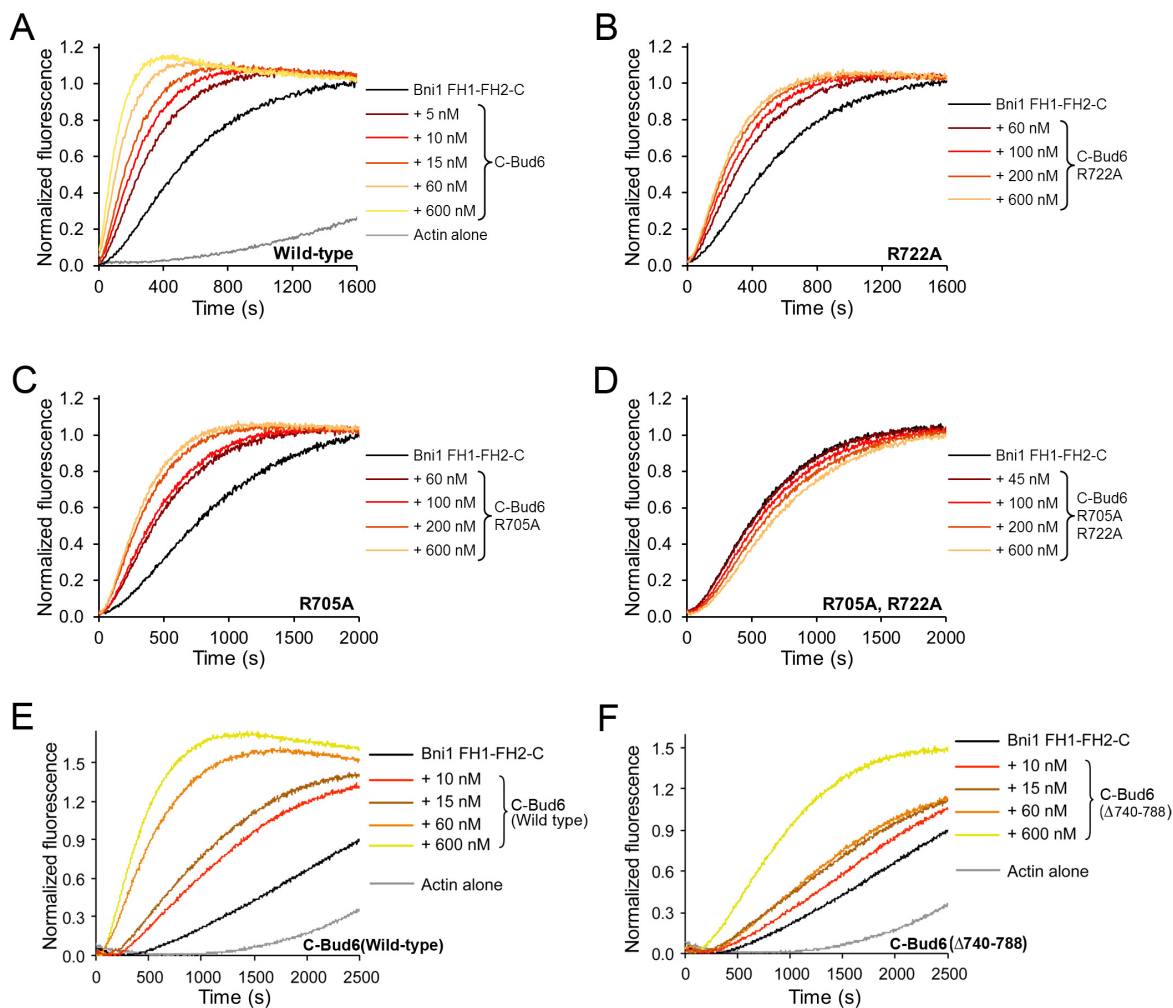


**Figure S3. Structure-function analysis of the Bud6-actin interaction. related to Figure 3.**

2  $\mu$ M monomeric actin was polymerized in the presence of 10 nM Bni1 FH1-FH2-C and indicated concentrations of C-Bud6. These are the raw data underlying Figure 3 in the main text. A-D, Actin assembly curves for wild type or mutant C-Bud6, (corresponding to Figure 3A). E and F, Actin assembly curves for intact C-Bud6 (residues 550-788) versus truncated C-Bud6 $\Delta^{740-788}$  (residues 550-739, corresponding to Figure 3B).